Reversible Color Changes in Lamella Hybrids of Poly(diacetylenecarboxylates) Incorporated in Layered Double Hydroxide Nanosheets

Toshio Itoh,[†] Tetsuya Shichi,[‡] Tatsuto Yui,[†,§] Hiroki Takahashi,[†] Yoshihisa Inui,[†] and Katsuhiko Takagi*[,†,§]

Department of Crystalline Materials Science, Graduate School of Engineering, Nagoya University, Chikusa-ku, Nagoya 464-8603, Japan, Central Japan Railway Company, Komaki, Aichi 485-0801, Japan, and CREST, JST (Japan Science and Technology), Japan

Received: October 7, 2004; In Final Form: December 10, 2004

The present study is an investigation of a reversible thermal color change induced in lamella hybrids of poly(diacetylenecarboxylates) incorporated in layered double hydroxide (LDH) nanosheets. These **poly-[*m,n*]/LDH** hybrids prepared by the photo- or γ-ray-induced polymerization of diacetylenecarboxylates, i.e., $CH_3(CH_2)_{m-1}C{\equiv}C-C{\equiv}C(CH_2)_{n-1}CO_2^-$ **(mono-[*m,n*])**, and intercalated in LDH lamella sheets, were observed to develop colors ranging from yellow to blue. The change in color was found to depend greatly on the alkyl carbon numbers of the **mono-[*m,n*]** (*m,n* = 10,11; 5,11; 10,5; 16,1) values. Moreover, the conformational alignment of the **mono-[*m,n*]** within the LDH was observed to be a crucial factor in color development, which was greatly affected by the intercalation degrees and extent of poly(ene-yne) linkage elongation of the polymers. For the **poly-[*m,n*]/LDH** hybrids investigated, a reversible color change was found to occur repeatedly and remarkably for the **poly-[10,11]/LDH** hybrid. This color change occurred at temperatures between ca. 20 and 80 °C back and forth from purple red to bright orange, in stark contrast to the irreversible color change for **poly-[10,11]** without LDH. Moreover, DSC and Raman spectroscopic studies of the LDH hybrids showed that the thermochromic temperature corresponded to the phase transition temperature of 80 °C. XRD analysis also indicated that the **poly-[*m,n*]/LDH** hybrid could retain its lamella structure during such thermochromic color changes, enabling conformational recovery in the polymer chains by a cooling down of the hybrids to temperatures lower than the transition temperature, while the nonhybrid **poly-[10,11]** powders exhibited an irreversible color change at 60 °C, above which the polymer powder turned amorphous.

Introduction

Diacetylene compounds are reported to be easily polymerized by either heat treatment or irradiation by ultraviolet light or γ-rays, as was first observed by Wegner et al.[1,2] Since then, there have been many studies in poly(diacetylenes) due to their multi-functional properties such as electroconductivity,[3,4] their third-order nonlinear optical characteristics,[5] thermochromism,[6−8] photochromism,[9] solvatochromism,[6] and ionic sensory properties, etc.[10]

Efficient chromatic changeability, a particularly promising property for photofunctional and optical systems, was found to be closely related not only to the extent of the conjugation over its polymerization backbone but also to the conformations of the side chains of the substituents within the polymer backbone.[11] It has been reported that long alkyl chains, linked to the poly(diacetylenes) main chains and contributing to their aggregation, are the main factors involved in the blue coloring attributed to supramolecular conformations as well as the widespread conjugation of the poly(diacetylene) backbones.[12−14] Indeed, in contrast to this, only a yellow to orange-yellow coloring appears for the weakly aggregated poly(diacetylenes) attributed to the short poly(diacetylene) conjugations.

Hybrid host materials which are able to accommodate inorganic or organic compounds into its interlayers would make it possible to develop materials that could retain the poly(diacetylene) chains anisotropically on substrates of any form or shape. On the basis of our previous study on layered double hydroxide (LDH) hybrids with long alkyl chained carboxylates,[15,16] inorganic lamella sheets showed great potential for the anisotropically accommodated poly(diacetylenes). Moreover, to the best of our knowledge, this is the first study on poly(diacetylenes) hybridized in inorganic lamella nanosheets such as LDH clay. Here, LDH is a typical layered anion-exchange clay referred to by its chemical formula, $Mg_{4.5}Al_2(OH)_{13}Cl_2{\cdot}3.5H_2O$, which possesses an anion exchange capacity (AEC) of 3.5 mequiv/g and is capable of accommodating anionic guest molecules in their interlayers which effectively create a balance with the positively charged layers.[17−22]

In the present study, we report on a novel method in which efficient repetition of a reversible color change for poly(diacetylenecarboxylates) LDH hybrids, i.e., **poly-[10,11]/LDH**, prepared by the polymerization of a series of diacetylenecarboxylates, $CH_3(CH_2)_{m-1}C{\equiv}C-C{\equiv}C(CH_2)_{n-1}CO_2H$ (**mono-[*m,n*]**), intercalated in LDH lamella sheets, could be initiated. Among the various poly(diacetylenecarboxylates)/LDH hybrids investigated, **poly-[10,11]/LDH** was found to exhibit the most efficient reversible thermochromism at 80 °C, in stark contrast to **poly-[10,11]** without LDH in which only an irreversible color

* To whom correspondence should be addressed. E-mail: ktakagi@apchem.nagoya-u.ac.jp.
† Nagoya University.
‡ Central Japan Railway Company.
§ CREST.

10.1021/jp045410e CCC: $30.25
Published on Web 02/08/2005

SCHEME 1: Synthesis of Diacetylenecarboxylates or Mono-[*m,n*]

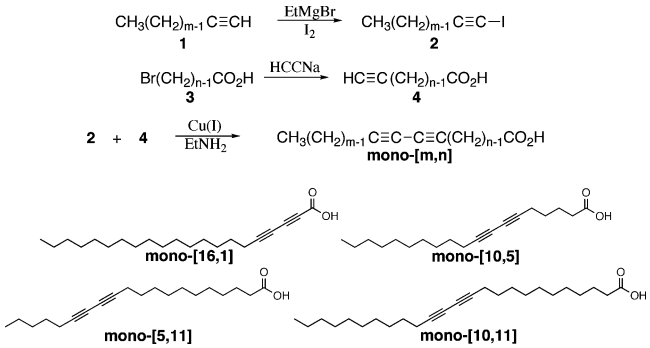

change at 60 °C accompanied by its irreversible change into an amorphous phase were observed.

Experimental Section

Synthesis of Diacetylenecarboxylic Acid, Mono-[*m,n*]. Diacetylenecarboxylic acids, **mono-[*m,n*]**, were prepared by the condensation of 1-iodo-1-aklynes (**1**) with ω-aklyne-1-carboxylic acids (**2**) by Cadiot−Chodkiewicz coupling in the presence of Cu(I) and ethylamine, as shown in Scheme 1 and detailed in previous literature.[23]

Mono-[5,11] was synthesized by the reaction of ω-tridecyn-1-oic acid (**2**, $n = 11$) with 1-iodo-1-heptyne (**1**, $m = 5$) obtained from the Grignard reagent of 1-heptyne with I_2 in accordance with procedures reported by Vaughn et al.[24] In a similar manner, **mono-[10,5]** and **mono-[10,11]** were synthesized by the reaction of 1-iodo-1-dodecyne (**1**, $m = 10$)[25] with ω-heptyn-1-oic acid (**2**, $n = 11$), respectively, while ω-tridecyn-1-oic acid (**2**, $n = 11$) was synthesized from 11-bromoundecanoic acid.[26−28] **Mono-[16,1]** is commercially available and was used with purification through an Advantec PTFE 0.20 μm pore size membrane filter (Tokyo Chemical Ind).

Measurement of the Surface Pressure−Area Isotherms of Mono-[*m,n*]. The surface pressure−area isotherms were measured with a Langmuir−Blödgett trough instrument (Nippon Laser & Electronics Laboratory, Model NL-LB200S-NWC). The surface pressure was monitored with a paper filter of 5 mm width as a Wilhelmy plate. A 20 μL solution of the diacetylenecarboxylic acids, **mono-[*m,n*]**, in chloroform was spread onto the ultrapure water surface (18 MΩ·cm^{-1}) in the trough and kept for 10 min to evaporate the chloroform under ventilated conditions. The isotherm profiles were recorded with use of a barrier running at a compression speed of 20 mm/min.

Synthesis of the Mono-[*m,n*]/LDH Hybrids. The sodium diacetylenecarboxylates, **mono-[*m,n*]**, were obtained by the addition of an equimolar amount of sodium methoxide in methanol, condensation by solvent evaporation, and then drying in vacuo for 3 h. An aqueous suspension of the **mono-[*m,n*]** (5 mmol·dm^{-3}) was prepared as a stock solution. Forty eight milliliters of the suspension including the amount of **mono-[*m,n*]** corresponding to 300% AEC was added to 22.9 mg of LDH and the solution was stirred magnetically for 5 days at 5 °C. The resulting hybrid precipitates were filtered and washed with ethanol, then dried in vacuo for 3 h to yield a series of LDH hybrid white powders: **mono-[10,5]/LDH**; **mono-[5,11]/LDH**; **mono-[16,1]/LDH**; and **mono-[10,11]/LDH**.

Estimation of the Amounts of Mono-[*m,n*] in the LDH Hybrids. Combustion analysis of the **mono-[*m,n*]/LDH** hybrids was carried out with a Perkin-Elmer 2400 series II CHNS/O analyzer. The results are summarized in Table 1.

TABLE 1: Combustion Analysis of Diacetylenecarboxylates/LDH Hybrids, Mono-[*m,n*]/LDH

	atom wt of C (%) at several added amounts					
	50%	100%	200%	250%	300%	350%
mono-[16,1]/LDH		38.8	38.1		37.7	
mono-[10,5]/LDH		36.8	40.8		44.2	
mono-[5,11]/LDH	23.6	35.6	46.2	48.0	48.7	
mono-[10,11]/LDH		45.9	58.8	59.5	61.3	61.3

Polymerization of Mono-[*m,n*] in the LDH Clays. The polymerization of the hybrids was carried out by UV light irradiation. All of the hybrid powders were placed in an area of 20 × 20 mm^2 on a quartz glass plate of 5 mm thickness and irradiated with UV light ($\lambda > 240$ nm), using a 300 W xenon lamp equipped with a cut filter (HOYA ultraviolet transmitting filters UV-25), at room temperature. This series of poly(diacetylenecarboxylates) is referred to as **poly-[10,5]**, **poly-[5,11]**, **poly-[16,1]**, and **poly-[10,11]**, while their corresponding polymerized LDH hybrids are referred to as **poly-[10,5]/LDH**, **poly-[5,11]/LDH**, **poly-[16,1]/LDH**, and **poly-[10,11]/LDH**, respectively.

X-ray Diffraction Analysis of the Hybrids. Powder X-ray diffraction analysis (XRD) of the **mono-[*m,n*]/LDH** hybrids was carried out with a Rigaku RINT-2100 XRD apparatus operating at 40 mA and 40 kV, and equipped with a Rigaku CN2173C3 goniometer set at 1.54 Å with Ni-filtered Cu Kα radiation as well as a Rigaku PTC-20A temperature controller. The XRD patterns were measured in the $2\theta/\theta$ mode within a 2θ range of 1.5−30° and a scan rate of 1 deg/min. The obtained data were collected five times and then averaged.

Electron Density Distribution. The electron density distributions along the *c*-axis in the alternatively stacked layer materials were calculated by means of a series of (00*l*) peaks of high periodicity.[29,30] On the basis of the electron density distribution, which is closely associated with the atom dispositions, the hybrid materials were characterized to exhibit a high regularity along the *c*-axis. Calculations were carried out with eq 1 and the Fourier transformations of the (00*l*) peaks in the XRD patterns of the hybrids, where l, $F(l)$, d, ϕ, and I denote the peak number (00*l*) of the diffraction order, the structural factor, layer distance, phase, and the peak area, respectively.

$$\rho(x) = \sum_{l=0}^{\infty} F(l) \cos\left(\frac{2\pi l x}{d}\right) \tag{1}$$

where

$$F(l) = \exp\{i\phi(l)\}|\sqrt{I(l)}|$$

The electron density of the LDH hybrids, $\rho^{\mathrm{T}}(x)$, was independently estimated with eq 2 by assuming the formation of bilayer structures composed of diacetylenecarboxylate ions in the interlayers. For eq 2, $F^{\mathrm{M}}(l)$ denotes the structural factor calculated from the electron density of the bilayer, $\rho^{\mathrm{M}}(x)$, as shown in Figure 6. $\rho^{\mathrm{M}}(x)$ was obtained by analyzing the electrons of all of the atoms constituting one unit layer.

$$\rho^{T}(x) = \sum_{l=1}^{l_{\max}} F^{\mathrm{M}}(l) \cos\left(\frac{2\pi l x}{d}\right) \tag{2}$$

where

$$F^{\mathrm{M}}(l) = \frac{2}{d}\int_0^d \rho^{\mathrm{M}}(x) \cos\left(\frac{2\pi l x}{d}\right) \mathrm{d}x$$

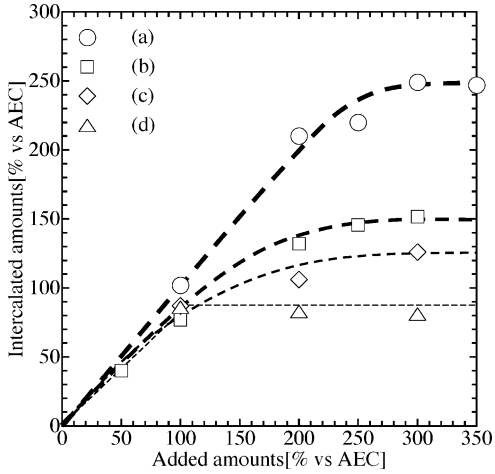

Figure 1. Intercalated amounts of **mono-[*m,n*]** against the added amounts: (a) **mono-[10,11]/LDH**; (b) **mono-[5,11]/LDH**; (c) **mono-[10,5]/LDH**; and (d) **mono-[16,1]/LDH**.

Diffuse Reflectance Spectroscopy Analysis of the Hybrids. The powdered samples (ca. 10 mg) were placed on a sample holder and their UV−vis absorption spectra were measured on a JASCO V-500 spectrophotometer equipped with either a JASCO ISV-469 diffuse reflectance unit or a heat treatment unit using a Peltier device with a direct current power source.

Differential Scanning Calorimetry of Poly-[*m,n*]/LDH Hybrids. The differential scanning calorimetry of the **poly-[*m,n*]** and **poly-[*m,n*]/LDH** hybrids was carried out with a differential scanning calorimeter by Seiko Instruments, DSC 6200. About 5 mg of each hybrid powder was placed into an aluminum vessel and heated from 0 to 140 °C at a rate of 5 deg/min under nitrogen atmosphere.

Raman Spectroscopic Analysis of the Hybrids. Raman spectroscopy of the **poly-[*m,n*]/LDH** hybrids was carried out with a Nihon Bunko NRS-1000 spectrometer equipped with a 532.3 nm laser operating at room temperature (ca. 20 °C).

Results and Discussion

Intercalation Degrees of mono-[*m,n*] in the LDH Interlayers. Depending on the **mono-[*m,n*]** variation, the intercalation degrees increased with an increase in the amounts of **mono-[*m,n*]** until a saturation point could be reached on the basis of the AEC of the LDH, as shown in Figure 1. It could be seen that the cross section of the **mono-[*m,n*]** unit molecule decreases with the addition of **mono-[*m,n*]**. For **mono-[10,11]**, saturation occurred at 20 Å^2 above 300% AEC, as calculated from the cross-section area of the all-trans alkyl chain,[31] 18.6 Å^2, and the lattice constant of the LDH. The average distance of the adjacent Al^{3+} ions on the LDH layer surface was 3.1 Å in the case of a Mg/Al ratio of ca. 2:1, where the unit area of the ion-exchange site was 50.6 Å^2, as shown in Figure 2,parts a and b.

In our previous work, the control of a number of aliphatic carboxylates, such as stearate ions, to self-assemble with the help of hydrophobic interactions within the LDH interlayers was investigated. The stearate ions could then form a bilayer assembly where the cross section was estimated at 22 Å^2/molecule.[16] In a similar manner, **mono-[10,11]** could be intercalated up to 250%, i.e., correspondent to the cross section of the 21 Å^2/molecule, while the intercalation for **mono-[16,1]** was inefficient and could only reach a saturation point at ca. 80% AEC.

The various **mono-[*m,n*]** investigated here were adsorbed into the LDH by the hydrophobic interactions of their alkyl chains.

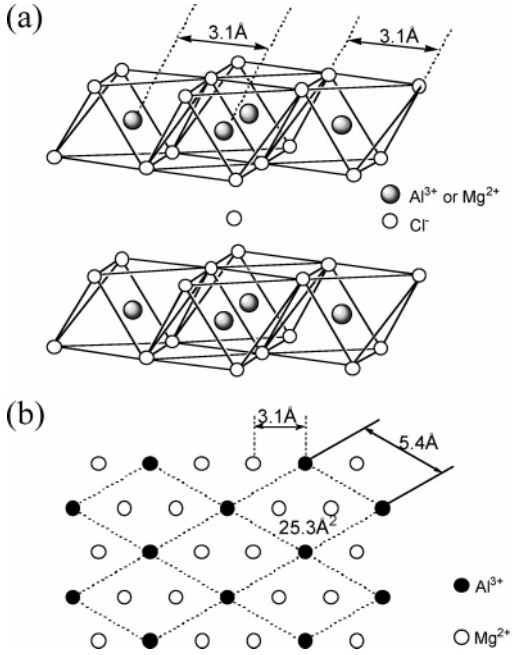

Figure 2. LDH frameworks: (a) lateral distance of about 3.1 Å for the octahedral unit; (b) arrangement of the metal cations in the octahedral units of the LDH framework. A space area of 50.6 Å^2 on both sides of the framework is depicted.

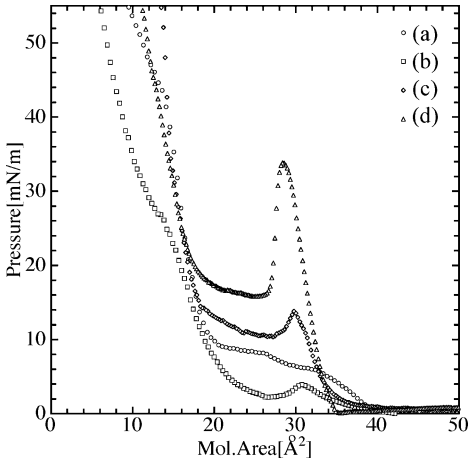

Figure 3. Surface pressure−area isotherms of **mono-[*m,n*]** measured at 5°C: (a) **mono-[10,11]**; (b) **mono-[5,11]**; (c) **mono-[10,5]**; and (d) **mono-[16,1]**.

For **mono-[10,11]**, the occupied area per molecule was 21 Å^2/molecule, indicating the formation of the most closely packed bilayers within the LDH interlayers and confirming efficient intercalation. The amount of **mono-[10,5]** and **mono-[5,11]** that could be intercalated into the LDH were only about half the **mono-[10,11]** that could be efficiently intercalated into the **mono-[10,11]/LDH** hybrid. **Mono-[16,1]** showed the least efficient intercalation, even though it possesses long alkyl chain substituents similar to those of the other diacetylenecarboxylates. The extent of the steric hindrance for the formation of molecular guest carboxylate aggregations in the LDH was evidenced by analysis of the $\pi-A$ curve. The existence of two discontinuous points indicating changes in the alignment could be observed upon increasing the surface pressure (π), as seen in Figure 3. **Mono-[16,1]** and **mono-[10,5]**, with short methylene chain spacers located between the carboxyl and diacetylene groups, steeply increased their surface pressures at the cross-section point of ca. 35 Å^2 per molecule, while **mono-[5,11]** and **mono-[10,11]** with long alkyl chains at the terminal position slowly

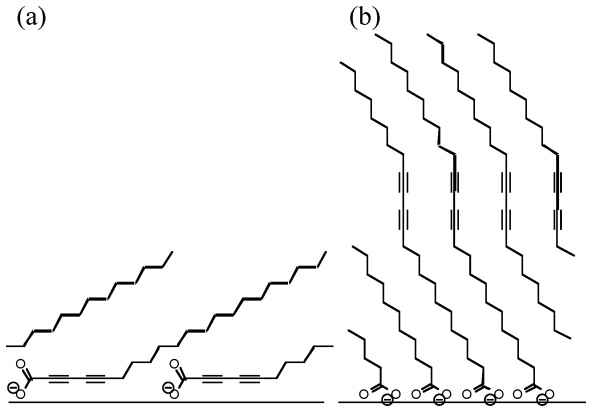

Figure 4. Alignment of **mono-[*m,n*]** on the water surface of the LB instrument: (a) **mono-[16,1]** and (b) **mono-[10,11]**.

and gradually increased their surface pressures at ca. 40 Å^2 per molecule, and then steeply increased again at ca. 20 Å^2, indicating little steric hindrance against the compressions when the diacetylene substituents first passed the point of abrupt change at ca. 40 Å^2.

The $\pi-A$ profiles depicted in Figure 3 correspond well to the intercalation efficiencies, as described above, so that **mono-[5,11]** and **mono-[10,11]** were shown to be more efficient than **mono-[16,1]** and **mono-[10,5]**. The two former diacetylenecarboxylates were, thus, found to be attractive materials that could induce the efficient formation of organized aggregates when incorporated into LDH clay. In contrast, since **mono-[16,1]** possesses a diacetylene group connected directly to the adjacent carboxylic group without the methylene spacers, only poorly organized aggregates could be formed due to the large cross section of the headgroup, as shown in Figure 4a. Analysis of the $\pi-A$ profiles showed **mono-[10,11]**, the most efficiently adsorbed in the LDH interlayers, to exhibit two kinds of aggregation structures, i.e., loosely and tightly packed conformations, as shown in Figure 3. Under conditions of saturated intercalation of ca. 250% AEC, the **mono-[10,11]/LDH** hybrid was found to have a bilayer unit structure, as shown in Figure 4b, and a good correlation between the cross sections of the present **mono-[10,11]/LDH** and our previously reported highly organized bilayer-structured stearate/LDH hybrids could be seen.[16]

Light-Induced Polymerization of Mono-[*m,n*]/LDH. The series of (00*l*) XRD peaks for the **poly-[*m,n*]/LDH** hybrid powders obtained after UV irradiation showed characteristic high periodic regularity of the polymer unit components, as can be seen in Figure 5. On the basis of these diffraction angles (00*l*), the interlayer distances (*d*) were calculated to be almost twice as long as the guest molecular lengths along the long or *c*-axis.

Among the **poly-[*m,n*]/LDH** hybrid powders investigated, **poly-[10,11]/LDH** was observed to show the sharpest and strongest intensities, without any contamination of the broad peak components (Figure 5a). Thus, **mono-[10,11]** is considered the most suitable model for a poly(diacetylene)-incorporated LDH hybrid, possessing the most closely packed and regularly oriented conformations. The estimated *d* values of the (00*l*) sharp peaks were in good accordance with the thickness of the **poly-[10,11]** bilayers. The electron density distributions of the hybrids were estimated by the relationship of $\rho(x)$ against x (eq 1), while $\rho^M(x)$, $\rho^T(x)$, and $\rho(x)$ represent the models for the electron density distributions, as shown in Figure 6, parts a, b, and c, respectively. The Fourier transformations (eq 2) were derived from the $\rho^M(x)$ model and the electron density distribution, as observed by the XRD (00*l*) peaks (eq 1).

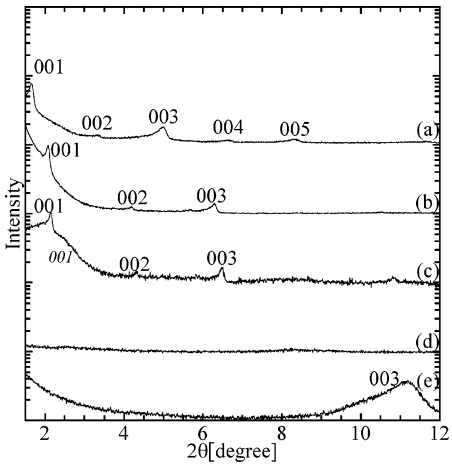

Figure 5. The X-ray diffraction patterns of the **poly-[*m,n*]/LDH** hybrids measured at ca. 20 °C: (a) **poly-[10,11]/LDH**; (b) **poly-[5,-11]/LDH**; (c) **poly-[10,5]/LDH**; (d) **poly-[16,1]/LDH**; and (e) Cl^- type LDH.

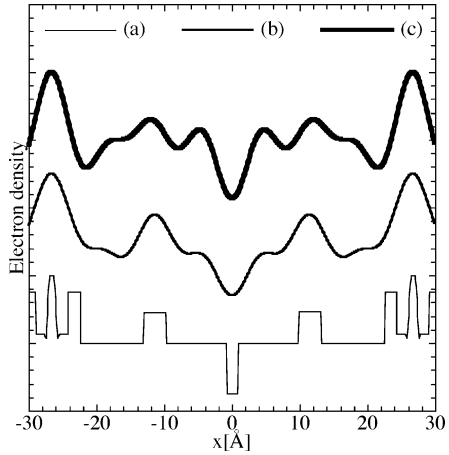

Figure 6. Electron density distribution of **poly-[10,11]/LDH** hybrid: (a) $\rho^M(x)$; (b) $\rho^T(x)$; and (c) $\rho(x)$.

Electron distribution analysis supported the view that the LDH hybrids consist of alternatively stacked units of a lamella bilayer sheet sandwiched by LDH octahedral lattice layers in which the OH^- ions are located together with the Al^{3+} and Mg^{2+} ions. Moreover, the obtained $\rho^T(x)$ reflects the high electron density distribution with a dip at the center, clearly indicating that the **mono-[10,11]** forms a bilayer lamella sheet within the interlayers.

Similarly to the **mono-[10,11]/LDH**, the **mono-[10,5]/LDH** hybrid powder exhibits XRD patterns of a mixture of two types of hybrid structures with broad and sharp diffraction peaks. The former broad signal is attributed to a monolayer conformation and the latter to a bilayer conformation, as with **mono-[10,11]**. The position of the diacetylene moieties has been noted to be an important factor in the highly organized self-assembly of the diacetylenecarboxylates within the LDH. In fact, as shown in Figure 5d, hardly any XRD peaks are observed, indicating the mostly random packing for the **mono-[16,1]/LDH** hybrid.

GPC analyses showed that the poly(diacetylenecarboxylate)s isolated from the **poly-[*m,n*]/LDH** hybrids (m,n = 10,5; 5,11; and 10,11) possess two maximum polymerization degrees (N_D) at ca. 30 and more than 100. Moreover, the content ratios for the higher N_D increased in the order of **poly-[10,5]/LDH**, **poly-[5,11]/LDH**, and **poly-[10,11]/LDH**. There is a similar tendency for the ratios of the bilayer/monolayer stacking structures for the corresponding **mono-[*m,n*]** in the LDH interlayers, as

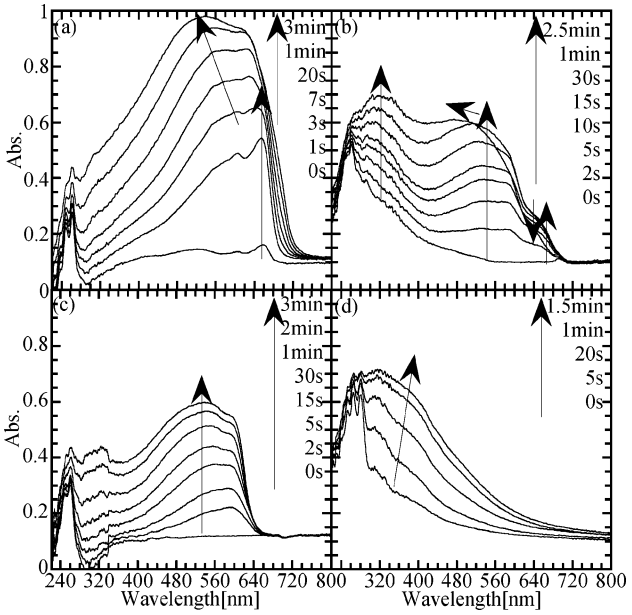

Figure 7. The successive diffuse reflectance spectral change of the poly(diacetylene-carboxylates) (**poly-[*m,n*]**) by UV irradiation: (a) **poly-[10,11]/LDH**; (b) **poly-[5,11]/LDH**; (c) **poly-[10,5]/LDH**; and (d) **poly-[16,1]/LDH**.

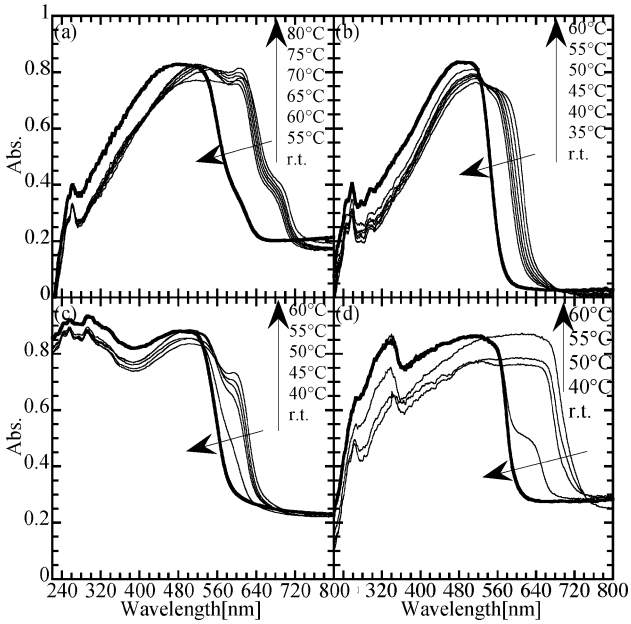

Figure 8. The successive diffuse reflection spectral changes for (a) **poly-[10,11]/LDH**, (b) **poly-[5,11]/LDH**, (c) **poly-[10,5]/LDH**, and (d) **poly-[10,11]** powders after appropriate time intervals, upon heating from ca. 20 to 80 °C.

observed by their XRD spectra. These results strongly suggest that the bilayer stacking conformation promotes the poly(ene-yne) polymerization more preferentially than a monolayer stacking alignment due to the proximity between the adjacent diacetylene groups. Thus, two kinds of structures for the **poly-[*m,n*]/LDH** hybrids, mono- and bilayer hybrids, were seen to be formed, and these structures were in good correspondence with the polymerization degrees, as detailed in the Supporting Information.

Figure 7 shows the diffuse reflectance absorption spectra for **poly-[*m,n*]/LDH** having various alkyl chain lengths with the total lengths almost constant. It is especially noteworthy that these UV-induced polymerized **poly-[*m,n*]/LDH** each possess a characteristic color, i.e., from pale yellow to blue, according to the position and the length of the poly(ene-yne)s in each of the molecules, as shown in Figure 7a−d.

These **poly-[*m,n*]/LDH** hybrids consisted of a series of colored components from yellow (λ_{max} = ca. 320 nm) through red (λ_{max} = ca. 500 nm) then purple (λ_{max} = ca. 580 nm) to blue (λ_{max} = ca. 640 nm) in variable ratios. The change in color for the **mono-[16,1]/LDH** hybrid was not very prominent and only a light orange appeared upon UV light illumination, indicating random alignment and, thus, leading to inefficient polymerization, whereas for the **mono-[10,5]/LDH** and **mono-[5,11]/LDH** hybrids, both clearly turned red upon polymerization. Small amounts of blue components could be observed for the **poly-[5,11]/LDH** so that it shows a weak absorption intensity in the blue region. A deep bathochromic shift of the absorption spectrum can be seen, remarkably for the case of the **poly-[10,-11]/LDH** hybrid, so that, upon polymerization, this hybrid mainly exhibited deep blue coloring due to its compactly packed alignment, which was seen to be more favorable for efficient polymerization. **Poly-[*m,n*]**, possessing long methylene chains between the carboxyl and diacetylene groups, were also observed to undergo bathochromic shifts in the absorption spectra, as can be seen in Figure 7a−d. The formation of the blue or red poly(diacetylenes) has been reported to be influenced by their intra- and intermolecular hydrogen bonding and the odd−even effect of the methylene groups.[12,13] In fact, the long methylene chain surfactant plays an important role in the aggregation of the guest diacetylene compounds and profoundly affects their conformations through strong hydrophobic−hydrophobic interactions in water. It could, thus, be observed that a well-oriented conformation is the main factor influencing efficient blue coloration.

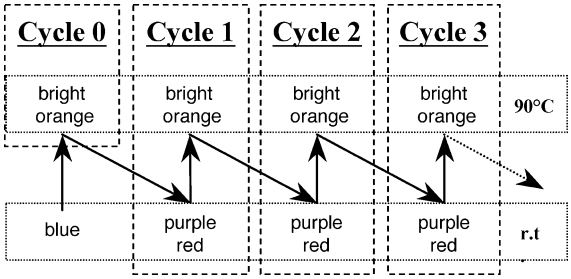

Figure 9. An outline of the alternative heating−cooling cycles of the **poly-[10,11]/LDH** hybrid. At the initial stage (Cycle 0), the color of the as-prepared hybrid is blue, and after Cycles 1−3, a reversible color change could be seen between purple-red and bright orange.

Reversible Color Changes for the Poly-[10,11]/LDH. Figure 8 shows that a blue to bright orange coloring could be observed upon heat treatment of the **poly-[*m,n*]/LDH** hybrids up to 80 °C. The **poly-[10,11]** itself without the LDH clay could only show an irreversible color change upon an increase in the temperature up to >60 °C, whereas the absorption spectra of the LDH hybrids gradually changed toward shorter wavelength regions by an increase in the temperature, then abruptly changed to bright orange at 80 °C.

Among the **poly-[*m,n*]/LDH** hybrids, a characteristic reversible thermal color change between purple and bright orange took place for the blue **poly-[10,11]/LDH**, as outlined in Figure 9. That is, the as-prepared **poly-[10,11]/LDH** powder changed its coloring from blue to bright orange upon heating to 80 °C at the first stage (Cycle 0). However, upon subsequent heating−cooling in Cycles 1−10, the color could be completely and reversibly changed between purple red and bright orange by alternatively changing the temperature between 90 °C and room temperature (ca. 20 °C), as shown in Figure 10. Moreover, in

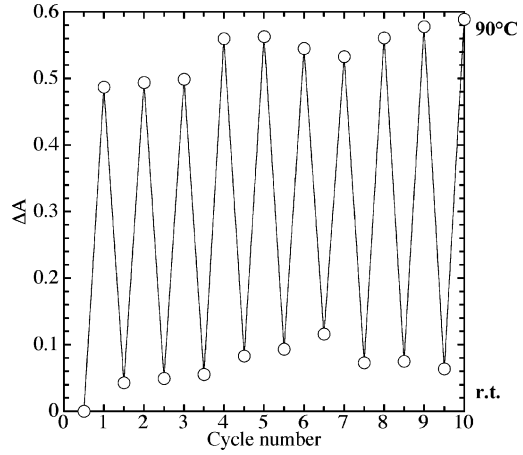

Figure 10. Reversible color changes in the **poly-[10,11]/LDH** hybrid. The absorbance at 575 nm could be completely and reversibly changed between purple-red and bright orange by alternatively changing the temperature between 90 °C and room temperature (ca. 20 °C).

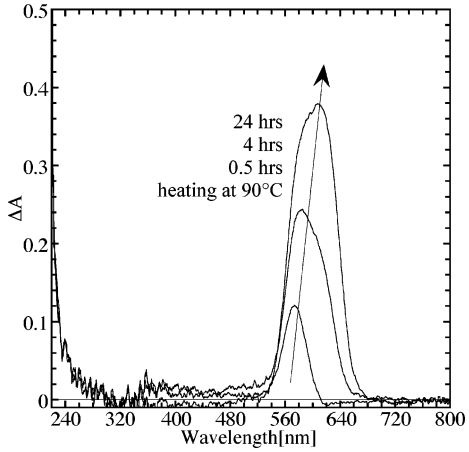

Figure 11. The color recovery in the subtraction spectra for the preheated **poly-[10,11]/LDH** hybrid upon cooling to ca. 20 °C.

an independent run, Figure 11 shows that the subtraction spectra of the bright orange **poly-[10,11]/LDH** could be seen at successive time intervals during a single cycle of the color change from bright orange to purple red upon cooling to room temperature, clearly indicating a color recovery of the purple red for the hybrids.

A thermal hypsochromic shift of the absorption maxima for the poly(diacetylenecarboxylates) in the hybrids can be attributed to (i) the disorder of the alignment of the poly(ene-yne)s in the LDH interlayers induced by a decrease in the electrostatic interaction of the carboxylate anions with the layer surfaces and/or (ii) the conformational degradation of the polymethylene chains in the poly(diacetylenecarboxylates) aggregates.

Relationship between the Color and Morphological Changes in the Poly-[10,11]/LDH. The morphological changes in the hybrids due to the thermal treatments are seen to induce the reversible color changes of the hybrids. In fact, DSC analysis showed a sharp phase transition due to the morphological changes in the hybrids, as shown in Figure 12. A number of researchers have reported the chromic changeability of poly(diacetylenes) to be induced by the conformational changes seen in the side alkyl chains of the polymer backbones.[32] To establish the conformational changes in the poly(diacetylenecarboxylates), the C≡C and C═C stretching vibrations in the range of around 2100 and 1500 cm^{-1}, respectively, of the Raman spectra for the hybrid **poly-[10,11]/LDH** hybrid were compared to those of the nonhybrid **poly-[10,11]** itself. As can be seen in Figure

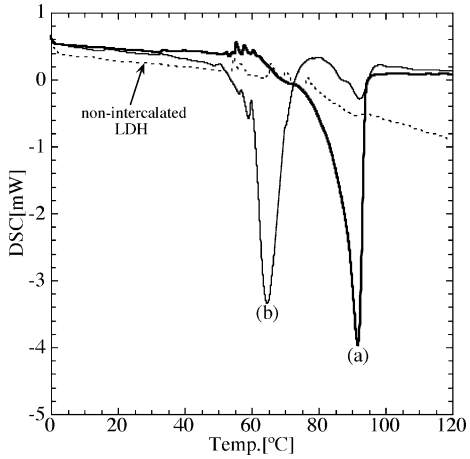

Figure 12. Differential scanning calorimetry charts of (a) **poly-[10,-11]/LDH** hybrid and (b) **poly-[10,11]** powders at 0 to 120 °C. The DSC chart of the nonintercalated LDH clay powder is shown for reference.

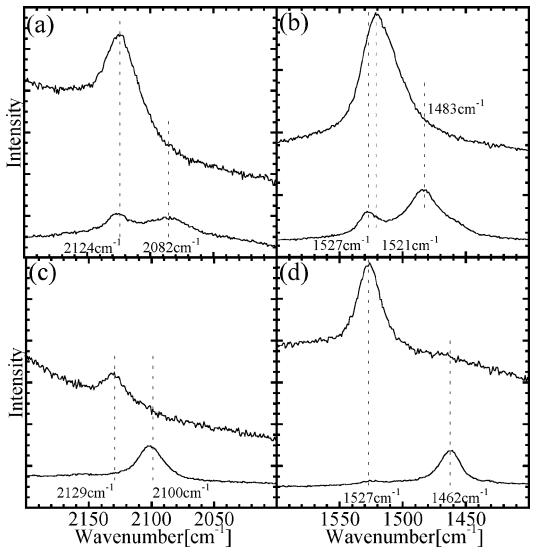

Figure 13. Raman spectra of the (a) C≡C stretching vibration and (b) C═C for the **poly-[10,11]/LDH** powder and the (c) C≡C stretching vibration and (d) C═C for the **poly-[10,11]** powder, measured with 532.3 nm excitation at room temperature. Upper and lower curves in each spectrum a−d represent before and after heat treatment at 90 °C, respectively.

13, for the former triple bond, the emission remains unchanged at 2124 cm^{-1} (Figure 13a); however, for the latter double bond, two emissions at 1527 and 1483 cm^{-1} shifted into one emission at 1521 cm^{-1} (Figure 13b). The newly appearing emission can be assigned to the conjugated poly(ene-ynes) conformations which were different from the original conformation. However, in contrast, the nonhybrid **poly-[10,11]** indicated irreversible and large shifts from 2100 to 2129 cm^{-1} (Figure 13c) and from 1462 to 1527 cm^{-1} (Figure 13d) for the carbon−carbon triple bond and the double bond emissions, respectively. These results clearly indicated that the LDH-supported **poly-[10,11]/LDH** had retained the ability for reversible color changes even upon heating at temperatures higher than 80 °C while a considerable and irreversible collapse of the conjugation for the nonhybrid **poly-[10,11]** was seen.

DSC analysis was carried out and the results clarified the thermal differences between the endothermic phase transitions of the **poly-[10,11]/LDH** hybrid and the nonhybrid **poly-[10,-11]**, as shown in Figure 12. The LDH hybrid exhibited a strong and sharp endothermic peak at ca. 92 °C, while the nonhybrid

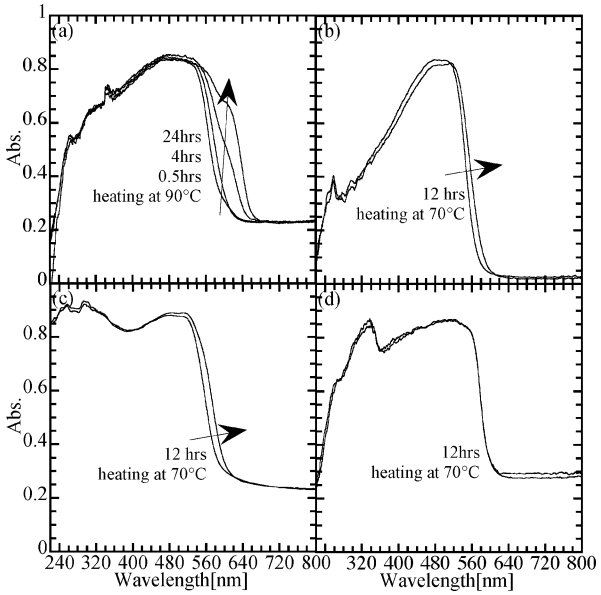

Figure 14. Diffuse reflection spectra of the reversed thermochromic process for (a) **poly-[10,11]/LDH** hybrid, (b) **poly-[5,11]/LDH** hybrid, (c) **poly-[10,5]/LDH** hybrid, and (d) **poly-[10,11]** powders upon a decrease in the temperature to an ambient ca. 20 °C.

poly-[10,11] mainly possessed a strong endothermic peak at ca. 65 °C accompanied by a second weak peak at 92 °C, respectively. Among these, the peak at ca. 92 °C may originate from the conformational changes of the organic guest molecules since they exist in the nonhybrid **poly-[10,11]** while no appreciable peaks from the LDH itself could be observed between 60 and 100 °C. The phase transition at ca. 92 °C showed a clear and good correspondence with the sudden change in color from blue to bright orange at around 80 °C. In contrast, the nonhybrid **poly-[10,11]** completely transformed its morphology at temperatures lower than 92 °C since the polymer chains were loosely packed without a supporting LDH framework. This could be understood not only by the effect of the heat treatment on the shifts in the C═C and C≡C stretching vibrations for the Raman spectroscopy but also by the fact that there was no IR absorption observed for the out-of-plane deformation vibrations (ωCH_2 and τCH_2) of the methylene chains, as detailed in the Supporting Information.

It is also interesting to note the differences in the enthalpies for the LDH hybrid **poly-[10,11]/LDH** and the nonhybrid **poly-[10,11]**. DSC analysis showed that the former LDH hybrid polydiacetylene possesses an enthalpy of 103 J/g by considering a weight of 76.5 wt % for the polymer component in the hybrid while the latter nonhybrid possesses an enthalpy of 172.1 J/g. The estimated enthalpy difference for the hybrid (ca. 70 J/g) indicates that it is more stable than the nonhybrid due to the closely packed conformation of the polymer backbone and alkyl chains in the LDH layers by the electrostatic fixation on the LDH surface.

Upon cooling the **poly-[10,11]/LDH** hybrid to room temperature, the blue coloring was gradually seen to recover and a reversible color change could be repeated between the temperatures of 20 and 90 °C, as shown in Figure 14. Moreover, the **poly-[5,11]/LDH** and **poly-[10,5]/LDH** hybrids underwent similar reversibility in color, though it was not as clear or efficient as the **poly-[10,11]/LDH**. It could, thus, be confirmed that the LDH clay layers firmly supported the morphological structures of the hybrids so that they would not collapse.

The thermochromism of the **poly-[10,11]/LDH** hybrid was observed to be accompanied by reversible morphological

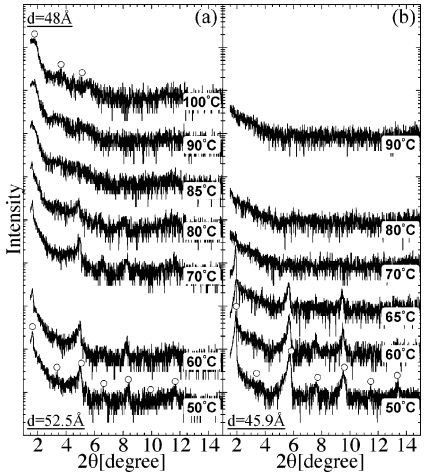

Figure 15. The morphological changes seen by monitoring the temperature-dependent XRD patterns: (a) **poly-[10,11]/LDH** hybrid and (b) **poly-[10,11]** powders.

SCHEME 2: Simplified Drawings of the Morphological Changes in the Lamella Unit Conformations upon Heat Treatment of (a) Poly-[10,11]/LDH Hybrid and (b) Poly-[10,11]

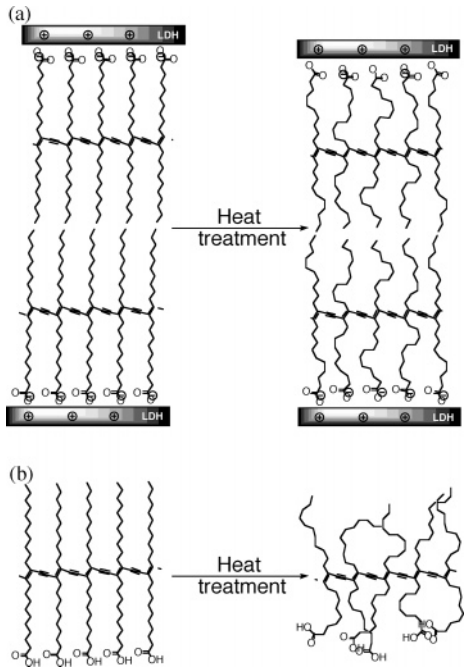

changes, as supported by results of the temperature-dependent XRD signals. In fact, the XRD profiles show that the lamella structure could be retained even at elevated temperatures of up to 100 °C, as shown in Figure 15a, while the nonhybrid **poly-[10,11]** already begins to collapse into an amorphous powder at around 70 °C (Figure 15b). The poly(diacetylenecarboxylates) lamella sheets in the **poly-[10,11]/LDH** hybrid could be seen to be strengthened and stabilized within the rigid sandwich framework when it forms with the alumina-magnesia octahedral sheets in the LDH clays. Scheme 2a,b clearly depict how the LDH hybrid is more thermally stable than its non-LDH counterpart.

Conclusions. LDH clay hybrids of poly(diacetylenecarboxylates) or **poly-[*m*,*n*]/LDH** were formed upon polymerization by UV light or γ-ray irradiation, and among the various hybrids investigated here, the **poly-[10,11]/LDH** hybrid powder showed the most highly uniform lamella bilayer unit structure as well

as the most efficient thermal reversibility. For the starting **mono-[*m,n*]** (*m,n* = 10,11; 5,11; 10,5; 16,1), polymerization induced color changes in varying degrees from light orange to red, purple, and finally blue depending on the alkyl chain carbon numbers. The alignment of **mono-[*m,n*]** was shown to play an important role in the coloration so that the **poly-[*m,n*]/LDH** hybrids which possessed long alkyl chains for both the *m* and *n* were seen to change most efficiently to blue. Moreover, **poly-[10,11]/LDH** was found to display a reversible thermal color change between purple and bright orange, in stark contrast to the irreversible, one-way color change seen for the **poly-[10,-11]** itself without LDH. The temperature at which the reversible color change occurred corresponded with the phase transition temperature of 80 °C, as shown by DSC analysis. Moreover, the phase transition reflects the reversible conformational changes of the alkyl chains even while the lamellar structure could be retained, as observed by analysis of the XRD diffraction peaks, in stark contrast to **poly-[*m,n*]** without LDH clay. The nonhybrid **poly-[10,11]** showed only an irreversible phase transition at 60 °C, above which the polymer powder turned amorphous. In conclusion, we have successfully prepared a novel poly(diacetylenecarboxylate) LDH hybrid, i.e., **poly-[10,11]/LDH**, showing unique superiority in retaining its lamella guest structure while enabling stable thermochromism, an attractive property for the development of organic−inorganic hybrid materials for advanced photofunctional and optical systems.

Acknowledgment. This work was partly supported by a Grant-in Aid for Scientific Research on Priority Areas (417) and the 21st Century COE Program "Nature-Guided Materials Processing" of the Ministry of Education, Science, Culture and Sports, Science and Technology (MEXT) of Japan. We would like to express our appreciation for their kind support. Thanks are also extended to CREST (Core Research for Evolutional Science and Technology) of JST (Japan Science and Technology Corporation) for their invaluable support.

Supporting Information Available: Experimental details with figures including diffuse reflectance spectra, X-ray diffraction patterns, IR absorption spectra, a GPC chart of the diacetylenecarboxylate/LDH hybrids, and differential scanning calorimetry charts. This material is available free of charge via the Internet at http://pubs.acs.org.

References and Notes

(1) Schott, M.; Wegner, G. *Nonlinear Optical Properties of Organic Molecules and Crystals*; Academic Press INC: New York, 1987; Vol. 2, p 3.
(2) Tieke, B. *Adv. Polym. Sci.* **1985**, *71*, 79.
(3) Shimada, S.; Masaki, A.; Matsuda, H.; Okada, S.; Nakanishi, H. *Mol. Cryst. Liq. Cryst.* **1998**, *315*, 385.
(4) Aida, T.; Tajima, K. *Angew. Chem.* **2001**, *113*, 3919.
(5) Sarkar, A.; Okada, S.; Matsuzawa, H.; Matsuda, H.; Nakanishi, H. *J. Mater. Chem.* **2000**, *10*, 819. Nakanishi, H. *Kikan Kagaku Sosetsu*; Japan Scientific Societies Press: Tokyo, Japan, 1992; Vol. 15, Chapter 6.
(6) Lu, Y.; Yang, Y.; Sellinger, A.; Lu, M.; Huang, J.; Fan, H.; Haddad, R.; Lopez, G.; Burns, A. R.; Sasaki, D. Y.; Shelnutt, J.; Brinker, C. J. *Nature* **2001**, *410*, 913. Yang, Y.; Lu, Y.; Lu, M.; Huang, J.; Haddad, R.; Xomeritakis, G.; Liu, N.; Malanoski, A. P.; Sturmayr, D.; Fan, H.; Sasaki, D. Y.; Assink, R. A.; Shelnutt, J. A.; Swol, F.; Lopez, G. P.; Burns. A. R.; Brinker, C. J. *J. Am. Chem. Soc.* **2003**, *125*, 1269.
(7) Tamura, H.; Mino, N.; Ogawa, K. *Thin Solid Films* **1989**, *179*, 33.
(8) Ahn, D. J.; Chae, E.; Lee, G. S.; Shim, H.; Chang, T.; Ahn, K.; Kim, J. *J. Am. Chem. Soc.* **2003**, *125*, 8976.
(9) Seki, T.; Tanaka, K.; Ichimura, K. *Polym. J.* **1998**, *30*, 646.
(10) Kolusheva, S.; Shahal, T.; Jelinek, R. *J. Am. Chem. Soc.* **2000**, *122*, 776.
(11) Saito, A.; Urai, Y.; Itoh, K. *Langmuir* **1996**, *12*, 3938.
(12) Huo, Q.; Russell, K. C.; Leblanc, R. M. *Langmuir* **1999**, *15*, 3972.
(13) Menzel, H.; Horstmann, S.; Mowery, M. D.; Cai, M.; Evans, C. E. *Polymer* **2000**, *41*, 8113.
(14) Cheadle, E. M.; Batchelder, D. N.; Evans, S. D.; Zhang, H. L.; Fukushima, H.; Miyashita, S.; Graupe, M.; Puck, A.; Shmakova, O. E.; Colorado, R., Jr.; Lee, T. R *Langmuir* **2001**, *17*, 6616.
(15) Kanoh, T.; Shichi, T.; Takagi, K. *Chem. Lett.* **1999**, 117.
(16) Itoh, T.; Ohta, N.; Shichi, T.; Yui, T.; Takagi, K. *Langmuir* **2003**, *19*, 9120.
(17) Frondel, C. *Am. Mineral.* **1941**, *26*, 295.
(18) Kanezaki, E. *J. Mater. Sci.* **1995**, *30*, 4926.
(19) Kuk, W.; Huh, Y. *J. Mater. Chem.* **1997**, *7*, 1933.
(20) Velu, S.; Sabde, D. P.; Shah, N.; Sivasanker, S. *Chem. Mater.* **1998**, *10*, 3451.
(21) Velu, S.; Suzuki, K.; Kapoor, M. P.; Tomura, S.; Ohashi, F.; Osaki, T. *Chem. Mater.* **2000**, *12*, 719.
(22) Rivers, V.; Kannan, S. *J. Mater. Chem.* **2000**, *10*, 489.
(23) Tieke, B.; Wegner, G.; Naegele, D.; Ringsdorf, H. *Angew. Chem., Int. Ed. Engl.* **1976**, *15*, 764.
(24) Vaughn, T. H. *J. Am. Chem. Soc.* **1933**, *55*, 3453.
(25) Svatos, A.; Saman, D. *Collect. Czech. Chem. Commun.* **1997**, *62*, 1457.
(26) DeJarlais, W. J.; Emken, E. A. *Synth. Commun.* **1980**, *10*, 653.
(27) Singh, A.; Schnur, J. M. *Synth. Commun.* **1986**, *16*, 847.
(28) Newton, R. F.; Pauson, P. L.; Taylor, R. G. *J. Chem. Res.* **1980**, 3501.
(29) Zeng, X.; Unger, G. *Polymer* **1998**, *19*, 4523.
(30) Adachi, T.; Takahashi, H.; Ohki, K.; Hatta, I. *Biophys. J.* **1995**, *68*, 1850.
(31) Kitaigorodsky, A. I. *Molecular Crystals and Molecules*; Academic Press: New York, 1973; Chapter 1.
(32) Exarhos, G. J.; Risen, W. M.; Baughman, R. H. *J. Am. Chem. Soc.* **1976**, *98*, 481.